Continuous Phase Modulation—Part I: Full Response Signaling

TOR AULIN, MEMBER, IEEE, AND CARL-ERIK W. SUNDBERG, MEMBER, IEEE

Abstract—**The continuous phase modulation (CPM) signaling scheme has gained interest in recent years because of its attractive spectral properties. Data symbol pulse shaping has previously been studied with regard to spectra, for binary data and modulation index 0.5. In this paper these results have been extended to the M-ary case, where the pulse shaping is over a one symbol interval, the so-called full response systems. Results are given for modulation indexes of practical interest, concerning both performance and spectrum. Comparisons are made with minimum shift keying (MSK) and systems have been found which are significantly better in E_b/N_0 for a large signal-to-noise ratio (SNR) without expanded bandwidth. Schemes with the same bit error probability as MSK but with considerably smaller bandwidth have also been found. Significant improvement in both power and bandwidth are obtained by increasing the number of levels M from 2 to 4.**

I. INTRODUCTION

FOR digital transmission over bandlimited channels, the demand for bandwidth efficient constant envelope signaling schemes with good reliability has increased in recent years. A system often used in practice is multilevel phase shift keying, M-ary PSK, which has the drawback that, although, for M equal 2 or 4, the receiver sensitivity is acceptable, the signal is too wide-band because of discontinuous phase. Thus, RF-filtering has to be performed before transmission causing a nonconstant envelope signal and a decreased receiver sensitivity. The so-called minimum shift keying (MSK), or fast frequency shift keying (FFSK), binary signaling schemes opened new prospects since the error probability performance is the same as coherent 2- or 4-ary PSK but the spectrum is narrower for large frequencies. Choosing an M larger than 4 (e.g., $M = 8$ or $M = 16$) in the MPSK system makes the main lobe of the spectrum narrower, but the sensitivity to noise is considerably increased.

A general definition of continuous phase modulation (CPM) systems is given in the next section. Assume that each data symbol only affects the instantaneous frequency of the transmitted signal in one symbol interval and that the phase is a continuous function of time. This defines the subclass full response CPM systems considered in this paper. In Part II more general CPM schemes are considered. In some cases the phase is allowed to be discontinuous while maintaining the coupling between the phase in successive symbol intervals.

By increasing M, an interesting tradeoff between symbol error probability at large signal-to-noise ratio (SNR) and spectrum is achieved. This trade off is studied for modulation indexes of practical interest and also for systems where the instantaneous frequency is not constant over each symbol interval.

The channel noise is assumed to be additive, white Gaussian throughout the paper. The symbol error probability for an optimum detector at large SNR is calculated using the minimum Euclidean distance between any two signals in the signal space [3]. The optimum detector operates coherently, and due to the continuous phase, the detector must observe the received signal for more than one symbol interval to make a decision about a specific symbol [3].

Manuscript received March 19, 1980; revised September 19, 1980. This work was supported by the Swedish Board of Technical Development under Grant 79-3594.

The authors are with the Department of Telecommunication Theory, University of Lund, Fack, S-220 07 Lund, Sweden.

II. GENERAL SYSTEM DESCRIPTION

For CPM systems, the transmitted signal is

$$s(t, \alpha) = \sqrt{\frac{2E}{T}} \cos(2\pi f_0 t + \varphi(t, \alpha) + \varphi_0) \tag{1}$$

where the information carrying phase is

$$\varphi(t, \alpha) = 2\pi h \int_{-\infty}^{t} \sum_{i=-\infty}^{\infty} \alpha_i g(\tau - iT)\, d\tau; \qquad -\infty < t < \infty \tag{2}$$

and $\boldsymbol{\alpha} = \cdots \alpha_{-2}\ \alpha_{-1}\ \alpha_0\ \alpha_1 \cdots$ is an infinitely long sequence of uncorrelated M-ary data symbols, each taking one of the values

$$\alpha_i = \pm 1, \pm 3, \ldots, \pm(M-1); \qquad i = 0, \pm 1, \pm 2, \cdots \tag{3}$$

with equal probability $1/M$. (M is assumed even.)

E is the symbol energy, T is the symbol time, f_0 is the carrier frequency, and φ_0 is an arbitrary constant phase shift which without loss of generality can be set to zero in the case of coherent transmission.

The variable h is referred to as the modulation index, and the amplitude of the baseband pulse $g(t)$ is chosen to give the maximum phase change $\alpha h\pi$ radians over each symbol interval when all the data symbols in the sequence $\boldsymbol{\alpha}$ take the same value α. For implementation reasons, rational values of the modulation index h are used. This is discussed in some detail in Part II.

To have a CPM signal, the information carrying phase $\varphi(t, \boldsymbol{\alpha})$ is a continuous function of time t, which implies that the frequency baseband pulse $g(t)$ does not contain any im-

0090-6778/81/0300-0196$00.75

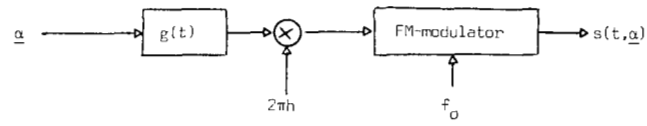

Fig. 1. Schematic modulator for CPM.

pulses. A schematic modulator is shown in Fig. 1. Note that a CPM signal always has a constant envelope.

Defining the baseband phase response (phase pulse)

$$q(t) = \int_{-\infty}^{t} g(\tau)\, d\tau; \qquad -\infty < t < \infty \tag{4}$$

it is seen that the phase of the CPM signal is formed by

$$\varphi(t, \alpha) = 2\pi h \sum_{i=-\infty}^{\infty} \alpha_i q(t - iT); \qquad -\infty < t < \infty. \tag{5}$$

A causal CPM system is obtained if the frequency pulse $g(t)$ satisfies

$$\begin{cases} g(t) \equiv 0; & t < 0, \quad t > LT \\ g(t) \not\equiv 0; & 0 \leqslant t \leqslant LT \end{cases} \tag{6}$$

where the pulse length L measured in symbol intervals T may be infinite. $L = 1$ yields full response schemes considered in this part. The normalizing constraint for the frequency pulse $g(t)$ can be expressed as

$$q(LT) = \tfrac{1}{2}. \tag{7}$$

The CPFSK modulation schemes [5], [7], [13] are a subclass of the CPM signaling scheme where the instantaneous frequency is constant over each symbol interval. Thus, for a full response CPFSK modulation scheme, we have

$$q(t) = \begin{cases} 0; & t \leqslant 0 \\ \dfrac{t}{2T}; & 0 \leqslant t \leqslant T \\ \tfrac{1}{2}; & t \geqslant T \end{cases} \tag{8}$$

which corresponds to linear phase trajectories over each symbol interval (see Fig. 2). Note that although the scheme is full response, the actual phase in any specific symbol interval depends upon the previous data symbols.

The CPM signal is assumed to be transmitted over an additive, white, and Gaussian channel having a one-sided noise power spectral density N_0. Thus, the signal available for observation is

$$r(t) = s(t, \alpha) + n(t); \qquad -\infty < t < \infty \tag{9}$$

where $n(t)$ is a Gaussian random process having zero mean and one-sided power spectral density N_0. A detector which minimizes the probability of erroneous decisions must observe the received signal $r(t)$ over the entire time axis and choose the

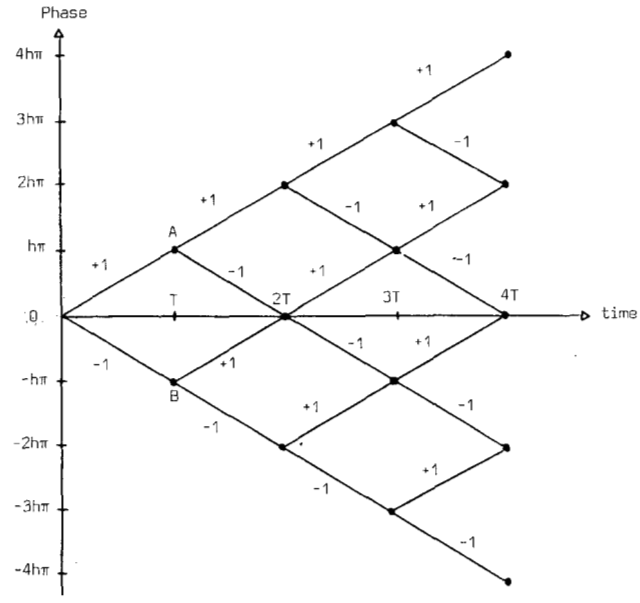

Fig. 2. Phase trajectories for a binary full response CPFSK system. Four bit time intervals are shown.

infinitely long sequence $\tilde{\alpha}$ which minimizes the error probability. This is referred to as maximum likelihood sequence estimation (MLSE). In order to be able to study the performance of an optimum MLSE detector, a suboptimum detector is studied instead. The limiting case of this suboptimum detector is the MLSE detector [7], [11].

This suboptimum detector observes the received signal $r(t)$ for N symbol intervals to make a decision about a specific data symbol, say α_0. Thus, the receiver observes the signal

$$r(t) = s(t, \alpha) + n(t); \qquad 0 \leqslant t \leqslant NT \tag{10}$$

and if we let $N \to \infty$, an MLSE detector is obtained. An optimum detector maximizes the likelihood function [3], [5]

$$\Lambda_N[r(t)] = e^{-\frac{2}{N_0}\int_0^{NT}[(r(t)-s(t,\tilde{\alpha})]^2\, dt} \tag{11}$$

and since the quantities $\int_0^{NT} r^2(t)dt$ and $\int_0^{NT} s^2(t, \tilde{\alpha})dt$ are independent of $\tilde{\alpha}_N = \tilde{\alpha}_0, \tilde{\alpha}_1, \cdots, \tilde{\alpha}_{N-1}$, one can, as well, maximize

$$\Lambda_N'[r(t)] = e^{\frac{2}{N_0}\int_0^{NT} r(t)s(t,\tilde{\alpha})\, dt} \tag{12}$$

or the log likelihood function

$$\log\,(\Lambda_N'[r(t)] = \int_0^{NT} r(t)s(t, \tilde{\alpha})\, dt. \tag{13}$$

Since there are M^N sequences, $\tilde{\alpha}_N = \tilde{\alpha}_0, \tilde{\alpha}_1, \cdots, \tilde{\alpha}_{N-1}$, but the detector is only interested in finding an estimate $\tilde{\alpha}_0$ of α_0, the M^N sequences can be formed into M groups:

$$\begin{cases} \tilde{\alpha}_{1,N}, \tilde{\alpha}_{3,N}, \cdots, \tilde{\alpha}_{(M-1),N} \\ \tilde{\alpha}_{-1,N}, \tilde{\alpha}_{-3,N}, \cdots, \tilde{\alpha}_{-(M-1),N} \end{cases} \tag{14}$$

where

$$\begin{cases} \tilde{\alpha}_{k,N} = k, \tilde{\alpha}_1, \tilde{\alpha}_2, \cdots, \tilde{\alpha}_{N-1} \\ k = \pm 1, \pm 3, \cdots, \pm(M-1) \end{cases} \tag{15}$$

and it is not necessary for the detector to find the specific sequence $\tilde{\alpha}_N$ which maximizes (13) and to choose $\tilde{\alpha}_0$ as an estimate of α_0. Instead, the detector must find which group of sequences $\tilde{\alpha}_{k,N}$, $k = \pm 1, \pm 3, \cdots, \pm(M-1)$ jointly maximizes (13), and take $\tilde{\alpha}_0$ as the group belonging. It is believed, however, that for large SNR the two detectors have the same performance [7].

The probability of an erroneous decision can be upper bounded by using the union bound [3], [5], [10]

$$P_e \leqslant \frac{1}{M^{N-1}} \sum_{\substack{k \\ k \neq l}} \sum_{l} Q\left[\frac{D(\alpha_{k,N}, \alpha_{l,N})}{\sqrt{2N_0}}\right] \tag{16}$$

where

$$Q(x) = \frac{1}{\sqrt{2\pi}} \int_x^\infty e^{-\frac{t^2}{2}}\, dt \tag{17}$$

and the summation is taken over all pairs of sequences defined by (15), with the restriction that $k \neq l$, $k, l = \pm 1, \pm 3, \cdots, \pm(M-1)$. $D[\alpha_{k,N}, \alpha_{l,N}]$ is the Euclidean distance between the signals $s(t, \alpha_{k,N})$ and $s(t, \alpha_{l,N})$.

The squared Euclidean distance can be written

$$\begin{aligned} &D^2(\alpha_{k,N}, \alpha_{l,N}) \\ &\quad = \int_0^{NT} [s(t, \alpha_{k,N}) - s(t, \alpha_{l,N})]^2\, dt \\ &\quad = \sum_{i=0}^{N-1} \int_{iT}^{(i+1)T} [s(t, \alpha_{k,N}) - s(t, \alpha_{l,N})]^2\, dt. \end{aligned} \tag{18}$$

Assuming $2\pi f_0 T \gg 1$, this can be written

$$\begin{aligned} &D^2(\alpha_{k,N}, \alpha_{l,N}) \\ &\quad = 2E\left(N - \frac{1}{T} \int_0^{NT} \cos\left[2\pi h \sum_{i=0}^{N-1} (\alpha_i^k - \alpha_i^l) \cdot q(t - iT)\right] dt\right). \end{aligned} \tag{19}$$

The superscript denotes the value of the first symbol in a sequence of N symbols, i.e.,

$$\begin{cases} \alpha_0{}^k = k \\ \alpha_i{}^k = \alpha_i; \qquad i = 1, 2, \cdots, N-1. \end{cases} \tag{20}$$

Equation (19) can be written

$$\begin{aligned} &D^2(\alpha_{k,N}, \alpha_{l,N}) \\ &\quad = 2E\left(N - \frac{1}{T} \int_0^{NT} \cos\left[\varphi(t, \alpha_{k,N} - \alpha_{l,N})\right] dt\right) \end{aligned} \tag{21}$$

Thus, it is sufficient to consider the difference sequence

$$\gamma_N = \alpha_{k,N} - \alpha_{l,N} \tag{22}$$

instead of the pair of sequences $\alpha_{k,N}$ and $\alpha_{l,N}$.

The approximation

$$P_e \approx \Gamma_0 \cdot Q\left[\frac{D_{\min,N}}{\sqrt{2N_0}}\right] \tag{23}$$

of (16) is good for large E/N_0. It is now assumed that E/N_0 is sufficiently large for this approximation to be valid. The limitations of this assumption is considered in detail in [20]. Γ_0 is a positive constant, independent of E/N_0, and $D_{\min,N}$ is the minimum of $D(\alpha_{k,N}, \alpha_{l,N})$ with respect to the pair of sequences $\alpha_{k,N}$ and $\alpha_{l,N}$ with the restriction that $k \neq l$. This quantity can also be calculated using the difference sequence γ_N through

$$D^2_{\min,N} = 2E \cdot \min_{\gamma_N} \left\{N - \frac{1}{T}\int_0^{NT} \cos\left[\varphi(t, \gamma_N)\right] dt\right\} \tag{24}$$

with the restriction that

$$\begin{cases} \gamma_0 = 2, 4, 6, \cdots, 2(M-1) \\ \gamma_i = 0, \pm 2, \pm 4, \cdots, \pm 2(M-1); \quad i = 1, 2, \cdots, N-1. \end{cases} \tag{25}$$

In Part II, we will only deal with squared Euclidean distances normalized by bit energy

$$d^2 = \frac{D^2}{2E_b} \tag{26}$$

Note that

$$E = E_b \cdot \log_2 (M) \tag{27}$$

where E_b is the bit energy. Thus, error probability comparisons for large SNR can be made directly in E_b/N_0 between systems even if they have different M. Only values that are powers of two ($M = 2, 4, 8, \cdots$) will be considered. As a reference point in the following, note that $d^2_{\min} = 2$ for MSK, binary PSK (BPSK), and quaternary phase shift keying (QPSK). For the case of full response CPFSK systems, calculations of $d^2_{\min,N}$ has been considered for both the bi-

nary case [1], [5]-[7], [13] and also for $M = 4$ and $M = 8$ to some extent [10], [11], [13].

III. BOUNDS ON THE MINIMUM EUCLIDEAN DISTANCE

An important tool for the analysis of CPM systems is the so-called phase tree. This tree is formed by all phase trajectories $\varphi(t, \alpha)$ having a common start value zero at $t = 0$. The ensemble is over the sequence α and Fig. 2 shows a part of the phase tree for a binary full response CPFSK system. A more general case is shown in Fig. 3 where two phase trees for a quaternary CPM system having different frequency baseband pulses $g(t)$ are shown.

To calculate the minimum squared Euclidean distance for an observation length of N symbols, all pairs of phase trajectories in the phase tree over N symbol intervals must be considered. The phase trajectories must not coincide over the first symbol interval however. The Euclidean distance is calculated according to (21) for all these pairs, and the minimum of these Euclidean distances is the desired result. It is of great importance to remember that the phase must always be viewed modulo 2π in conjunction with distance calculations. A practical method to do this is to form a cylinder by folding the phase tree [16], [17]. Trajectories which seem to be far apart in the phase tree might actually be very close or even coincide when viewed modulo 2π.

It is clear from (18) that, for a fixed pair of phase trajectories, the Euclidean distance is a nondecreasing function of the observation length N. If just a few pairs of infinitely long sequences are chosen, an upper bound on the minimum Euclidean distance at all values of the observation interval N is obtained. Good candidates for these infinitely long pairs are pairs that merge as soon as possible. Two phase trajectories merge at a certain time if they coincide all the time thereafter. These merges are called *inevitable* if they occur independently of h. Thus, an upper bound on the minimum Euclidean distance is obtained as a function of the modulation index h for all N.

Applying this method to the scheme in Fig. 2, it is seen that if a pair of sequences is chosen as

$$\begin{cases} \alpha_{+1} = +1, -1, \alpha_2, \alpha_3, \cdots \\ \alpha_{-1} = -1, +1, \alpha_2, \alpha_3, \cdots \end{cases} \tag{28}$$

the two phase trajectories coincide for all $t \geq 2T$. Thus, the upper bound on the normalized minimum squared Euclidean distance is

$$d_B^2(h) = 2 - \frac{1}{T} \int_0^{2T} \cos\left[2\pi h(2q(t) - 2q(t-T))\right] dt \tag{29}$$

where (21) was used. For the binary CPFSK system, i.e., linear phase trajectories, the result is

$$d_B^2(h) = 2\left(1 - \frac{\sin 2\pi h}{2\pi h}\right). \tag{30}$$

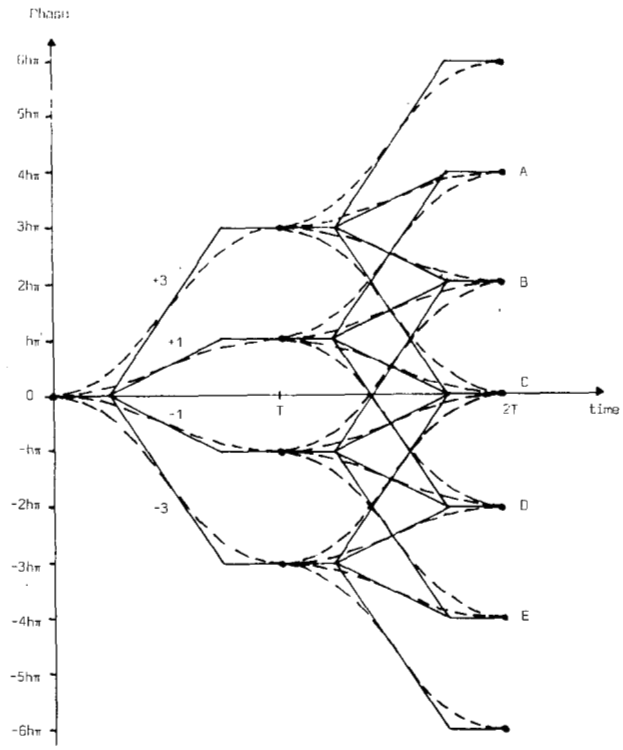

Fig. 3. Phase trees for $M = 4$ CPM schemes with two different baseband pulses $g(t)$. The α, β function [see (56)] with $\alpha = 0.25$, is $\beta = 0$ is shown by a solid line and the HCS, half cycle sinusoid [see (58)] is shown by a dashed line.

It can be noted that instead of using the pair of sequences (28), the single difference sequence $\gamma = +2, -2, 0, 0, \cdots$ could be used together with (24) for calculation of the normalized squared Euclidean distance.

Turning to the quaternary case, we can find pairs of phase trajectories merging at $t = 2T$. Fig. 3 shows two examples of phase trees for this case. These merges occur at the points labeled A, B, C, D, and E in the phase tree. Unlike the binary case, there is more than one merge point, and two different pairs of phase trajectories can have the same merge point. There are only three phase differences however, namely, those having phase difference $+2h\pi$, $+4h\pi$, and $+6h\pi$ at $t = T$.

It is easily seen that an upper bound on the minimum Euclidean squared distance for the M-ary case is obtained by using the difference sequences

$$\gamma = \gamma_0, -\gamma_0, 0, 0, 0; \qquad \gamma_0 = 2, 4, 6, \cdots, 2(M-1) \tag{31}$$

and taking the minimum of the resulting Euclidean distances, i.e.,

$$d_B^2(h) = \log_2 (M) \cdot \min_{1 \leq k \leq M-1} \left\{ 2 - \frac{1}{T} \int_0^{2T} \cos\left[2\pi h \cdot 2k(q(t) - q(t-T))\right] dt \right\} \tag{32}$$

which, for the M-ary CPFSK system, specializes to

$$d_B^2(h) = \log_2(M) \cdot \min_{1 \leq k \leq M-1} 2\left(1 - \frac{\sin k2\pi h}{k2\pi h}\right). \quad (33)$$

Fig. 4 shows the minimum distance $d^2(h)$ for binary CPFSK as a function of h and N. The upper bound d_B^2 is shown dashed. Note the peculiar behavior at $h = 1$. This will be discussed later.

It can be noticed that for all full response CPM systems with the property

$$\int_0^T g(\tau)\, d\tau = 0 \quad (34)$$

a merge can occur at $t = T$ and thus the difference sequences

$$\gamma = \gamma_0, 0, 0, 0, \cdots; \qquad \gamma_0 = 2, 4, 6, \cdots, 2(M-1) \quad (35)$$

yield the upper bound

$$d_B^2(h) = \log_2(M) \cdot \min_{1 \leq k \leq M-1} \left\{1 - \frac{1}{T}\int_0^T \cos\left[2\pi h \cdot 2q(t)\right] dt\right\}. \quad (36)$$

This class of pulses is called weak [20], and is not considered because distance properties are poor. Only positive pulses $g(t)$ will be considered below. Furthermore, they are assumed to be symmetric with

$$g(t) = g(T-t); \qquad 0 \leq t \leq T. \quad (37)$$

Weak Modulation Indexes, h_c

For the construction of the upper bound $d_B^2(h)$ on the minimum squared Euclidean distance, pairs of phase trajectories giving merges at $t = 2T$ were used. These merges occur independently of the value of h. For all pulses $g(t)$ except weak ones the first inevitable (for all h), merge occurs at $t = 2T$. For specific values of the modulation index h, however, other merges are also possible. In the binary case (see Fig. 2), a merge can occur at $t = T$ if the difference sequence is chosen to be $\gamma = +2, 0, 0, \cdots$ and the modulation index h is an integer. This is because the two points labeled A and B are a multiple of 2π apart, and thus coincide modulo 2π.

For an M-ary full response system, the phase trajectories take the values $\pm 2\pi hq(T)$, $\pm 6\pi hq(T)$, $\cdots$, $\pm 2(M-1)h\pi q(T)$, which for positive $g(t)$ pulses reduces to $\pm h\pi$, $\pm 3h\pi$, $\cdots$, $\pm(M-1)h\pi$. Thus, there are $M-1$ phase differences between the nodes in the phase tree at $t = T$, and merges occur at $t = T$ for h-values given by

$$\pi h \cdot \gamma_0 = 2\pi \cdot n; \quad \gamma_0 = 2, 4, 6, \cdots, 2(M-1) \qquad n = 1, 2, \cdots \quad (38)$$

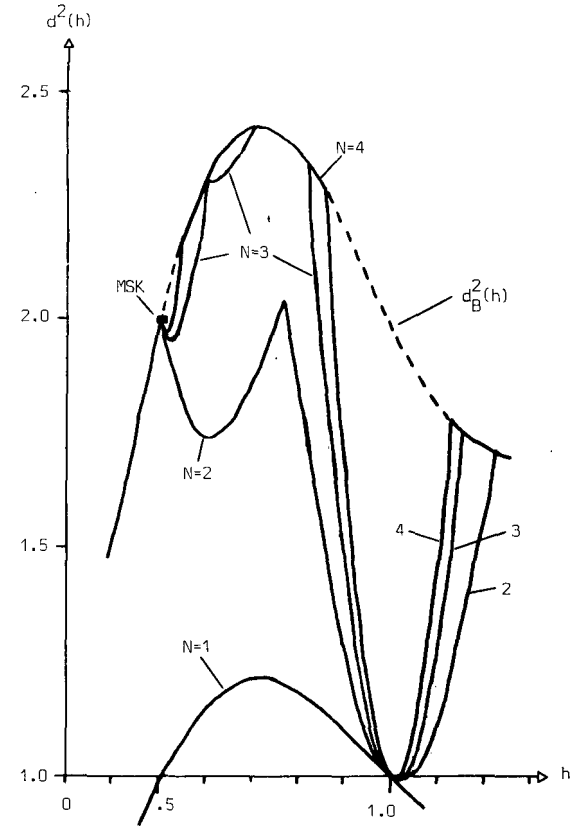

Fig. 4. Normalized squared Euclidean distance versus modulation index for binary CPFSK: upper bound (dashed line) and $d^2(h)$ for N = 1, 2, 3 and 4 bit decision intervals.

The modulation indexes [defined by (38)]

$$h_c = \frac{n}{k}; \qquad k = 1, 2, \cdots, M-1 \qquad n = 1, 2, \cdots \quad (39)$$

are called *weak* modulation indexes of the first order. For these modulation indexes, the minimum Euclidean distance is normally below the upper bound for all values of N; see Fig. 4 for $h = 1$. Sometimes the minimum distance for weak modulation index values is considerably below $d_B^2(h_c)$. For such cases, h_c is called a *catastrophic* modulation index value [17]-[20].

Merges of the weak (catastrophic) type occur at any observation length. Thus, weak h-values of the second order are defined by

$$\pi h(\gamma_0 + \gamma_1) = 2\pi \cdot n \qquad \gamma_0 = 2, 4, 6, \cdots, 2(M-1) \quad (40)$$
$$\gamma_1 = \pm 2, \pm 4, \pm 6, \cdots, \pm 2(M-1)$$
$$n = 1, 2, \cdots$$

As we will see later, the effect of weak modulation indexes of a higher order than one are of minor importance, since the corresponding Euclidean distance for the pairs of phase trajectories causing the merge is above the upper bound $d_B^2(h)$ [20]. For weak modulation indexes of the second order, the

corresponding Euclidean distance might be on the upper bound $d_B^2(h)$; for the third order and higher it is strictly above. But from (39) it can be seen that the number of first-order weak modulation indexes grows rapidly with M.

For weak modulation indexes of the first order, it is sufficient to calculate the corresponding Euclidean distance over the first symbol interval. Since the calculation of the upper bound uses the two first symbol intervals, it can be concluded that $d^2(h_c)$ can be, and normally is, smaller than $d_B^2(h_c)$. Thus, for weak modulation indexes of the first order, $d_{\min}^2(h_c)$ might be smaller than $d_B^2(h_c)$ (for details, see [20]). Furthermore, it is shown in detail [17], [20] that only h_c of the first order can influence the minimum distance calculation for full response CPM systems.

Tightness of the Upper Bound $d_B^2(h)$

A powerful property of the upper bound on the minimum Euclidean distance is that except for weak modulation indexes of the first order, the minimum Euclidean distance itself equals this bound if the observation interval is long enough [18], [20]. Denoting the minimum normalized squared Euclidean distance for an N symbol observation interval $d_{\min,N}^2(h)$, we have that

$$d_{\min,N}^2(h) = d_B^2(h) \tag{41}$$

if

$$\begin{cases} N \geq N_B(h) \\ h \neq h_c: \quad \text{(first order)}. \end{cases} \tag{42}$$

$N_B(h)$ is the number of symbol intervals required to reach the upper bound for the specific modulation index h.

If a specific pair of phase trajectories never merge, the Euclidean distance will grow without limit. This is true because the Euclidean distance calculated over each symbol interval is positive. Since the minimum distance was previously shown to be upper bounded, the pair of phase trajectories giving the minimum distance must eventually merge.

For a modulation index near a first-order weak modulation index, the difference sequence (35) gives the smallest growing Euclidean distance with N:

$$d^2(h) = \log_2(M) \min_{1 \leq k \leq M-1} \left\{ 1 - \frac{1}{T}\int_0^T \cos[2\pi h k \gamma_0 q(t)]\, dt + (N-1)(1 - \cos[\pi h k \gamma_0]) \right\} \tag{43}$$

and the smallest growth rate per symbol interval is

$$\log_2 M \cdot \min_{1 \leq k \leq M-1} \{1 - \cos[\pi h k \gamma_0]\}. \tag{44}$$

For sufficiently large N in (43), the minimum distance for the considered h is given by $d_B^2(h)$ since $d^2(h)$ will exceed $d_B^2(h)$.

The tightness of the upper bound and the behavior of (43) is illustrated in all the minimum distance figures.

Optimization of the Upper Bound $d_B^2(h)$

For frequency pulses $g(t)$ having the symmetry property (37), the expression for the upper bound can be written

$$d_B^2(h) = \log_2 M \min_{1 \leq k \leq M-1} \left\{ 2\left(1 - \frac{1}{T}\int_0^T \cos[4\pi h k q(t)]\, dt\right)\right\} \tag{45}$$

and since $\cos(\cdot) \geq -1$, $d_B^2(h)$ can never exceed $4 \cdot \log_2 M$. Thus, at most, an improvement of 3 dB in E/N_0 for a large SNR might be obtained for the binary case compared to MSK.

Furthermore, (45) can also be written

$$d_B^2(h) = \log_2 M \cdot \min_{1 \leq k \leq M-1} \left\{ 2\left(1 - 2\cos[\pi h k] \cdot \frac{1}{T}\int_0^{T/2} \cos[4\pi h k q_0(t) - \pi h k]\, dt\right)\right\} \tag{46}$$

where

$$q_0(t) = q(t + T/2). \tag{47}$$

The binary case ($M = 2$) will be considered first. In this case,

$$d_B^2(h) = 2\left[1 - 2\cos \pi h \cdot \frac{1}{T}\int_0^{T/2} \cos[4\pi h q_0(t) - \pi h]\, dt\right]. \tag{48}$$

It can at once be observed that $\cos \pi h = 0$ for $h = 1/2, 3/2, 5/2$, etc. Thus, the upper bound equals two, independent of the shape of the frequency pulse $g(t)$. Actually, this is true for all pulses $g(t)$ (except weak ones) [16]. This is of particular interest since much attention has been devoted to the case of $h = 1/2$ [6], [12], [14], [15].

To maximize $d_B^2(h)$ for the binary case, the last term in (48) must be minimized. Two different cases can be distinguished:

Case I:

$$0 \leq h \leq \tfrac{1}{2} \text{ where } \cos \pi h \geq 0. \tag{49}$$

Case II:

$$\tfrac{1}{2} \leq h \leq 1 \text{ where } \cos \pi h \leq 0. \tag{50}$$

To maximize $d_B^2(h)$, the integral in (48) must be minimized for case I and maximized for case II. It is also clear that the

pulse, which maximized $d_B^2(h)$ for case I, minimizes $d_B^2(h)$ for case II and vice versa.

To make the integral in (48) as small as possible, the argument inside the cosine must be as close to π as possible. This yields for the interval $0 \leqslant h \leqslant 1$

$$\begin{cases} q_0(t) = \frac{1}{2}; \text{ case I} \\ q_0(t) = \frac{1}{4}; \text{ case II} \end{cases} \tag{51}$$

with the resulting phase responses

$$q_1(t) = \begin{cases} 0; & 0 \leqslant t < \dfrac{T}{2} \\ \frac{1}{2}; & t > \dfrac{T}{2} \end{cases} \quad \text{case I} \tag{52}$$

and

$$q_2(t) = \begin{cases} 0; & t = 0 \\ \frac{1}{4}; & 0 < t < T \\ \frac{1}{2}; & t \geqslant T \end{cases} \quad \text{case II.} \tag{53}$$

From the sign symmetry, to minimize $d_B^2(h)$ the phase responses above have to be interchanged with each other for the respective cases.

The upper bound $d_B^2(h)$ for the two phase responses is now found as

$$\begin{cases} d_B^2(h) = 1 - \cos 2\pi h; & \text{using } q_1(t) \\ d_B^2(h) = 2(1 - \cos \pi h); & \text{using } q_2(t) \end{cases} \quad 0 \leqslant h \leqslant 1. \tag{54}$$

Thus, for any binary scheme, $d_B^2(h)$ is bounded by

$$\begin{cases} 1 - \cos 2\pi h \leqslant d_B^2(h) \leqslant 2(1 - \cos \pi h); & 0 \leqslant h \leqslant \frac{1}{2} \\ 2(1 - \cos \pi h) \leqslant d_B^2(h) \leqslant 1 - \cos 2\pi h; & \frac{1}{2} \leqslant h \leqslant 1. \end{cases} \tag{55}$$

An analogous technique can be used to derive bounds for $h \geqslant 1$.

The two phase responses $q_1(t)$ and $q_2(t)$ are members of the class called α, β functions [16], [17] defind by

$$q(t) = \begin{cases} \dfrac{\beta}{2\alpha}\dfrac{t}{T}; & 0 \leqslant t \leqslant \alpha T \\ \dfrac{\alpha}{2}\dfrac{t}{T}\dfrac{1-2\beta}{1-2\alpha} + \dfrac{\beta}{2}; & \alpha T \leqslant t \leqslant (1-\alpha)T \\ \dfrac{\beta}{2\alpha}\left(\dfrac{t}{T} - 1\right) + \frac{1}{2}; & (1-\alpha)T \leqslant t \leqslant T \\ \dfrac{1}{2}; & t \geqslant T. \end{cases} \tag{56}$$

Hence, when $h = 1/2$, $q_1(t)$ corresponds to binary PSK but with a $T/2$ time offset. The phase response $q_2(t)$ corresponds to a so-called plateau function; i.e., the phase changes only in the beginning and the end of the symbol interval, but remains constant (forms a plateau) in the middle of the symbol interval. Note that $q_1(t)$ and $q_2(t)$ give systems with discontinuous phase. However, the ensemble of possible phase trajectories is completely known to the receiver just as for all CPM systems. This gives a slight generalization of the considered class of systems.

It is interesting to note that the plateau function with $\beta = 1/2$ gives the upper bound [17]

$$d_B^2(h) = 2\left\{1 - (1-2\alpha)\cos \pi h - \frac{\alpha}{h\pi}\sin 2\pi h\right\} \tag{57}$$

which, for small values of α, approaches a value of 4 near $h = 1$. Since $h = 1$ is a first-order weak modulation index, it is concluded that large values of N are required to make $d_{\min}^2(h)$ equal $d_B^2(h)$ near $h = 1$.

In practice, the phase responses $q_1(t)$ and $q_2(t)$ are not attractive because of their spectra. This will be discussed more in Section VI. From a spectral point of view, the phase during a symbol interval should change slowly and smoothly, and the following frequency pulses with corresponding phase responses are of interest. The first one is

$$g(t) = \begin{cases} 0; & t \leqslant 0, t \geqslant T \\ \dfrac{\pi}{4T}\sin\dfrac{\pi t}{T}; & 0 \leqslant t \leqslant T \end{cases} \tag{58}$$

with the corresponding phase response

$$q(t) = \begin{cases} 0; & t \leqslant 0 \\ \frac{1}{4}\left(1 - \cos\dfrac{\pi t}{T}\right); & 0 \leqslant t \leqslant T \\ \frac{1}{2}; & t \geqslant T \end{cases} \tag{59}$$

and like CPFSK this pulse $g(t)$ has no continuous derivatives at the end points [14]. The pulse in itself is continuous, however, unlike CPFSK. Since the frequency pulse is a half cycle sinusoid, this scheme will be referred to as half cycle sinusoid (HCS) [see Fig. 3 (dashed tree) for the quaternary case].

Another pulse of interest is

$$g(t) = \begin{cases} 0; & t \leqslant 0, t \geqslant T \\ \dfrac{1}{2T}\left(1 - \cos\dfrac{2\pi t}{T}\right); & 0 \leqslant t \leqslant T \end{cases} \tag{60}$$

with the corresponding phase response

$$q(t) = \begin{cases} 0; & t \leqslant 0 \\ \dfrac{1}{2}\left(\dfrac{t}{T} - \dfrac{1}{2\pi}\sin\dfrac{2\pi t}{T}\right); & 0 \leqslant t \leqslant T \\ \dfrac{1}{2}; & t \geqslant T. \end{cases} \tag{61}$$

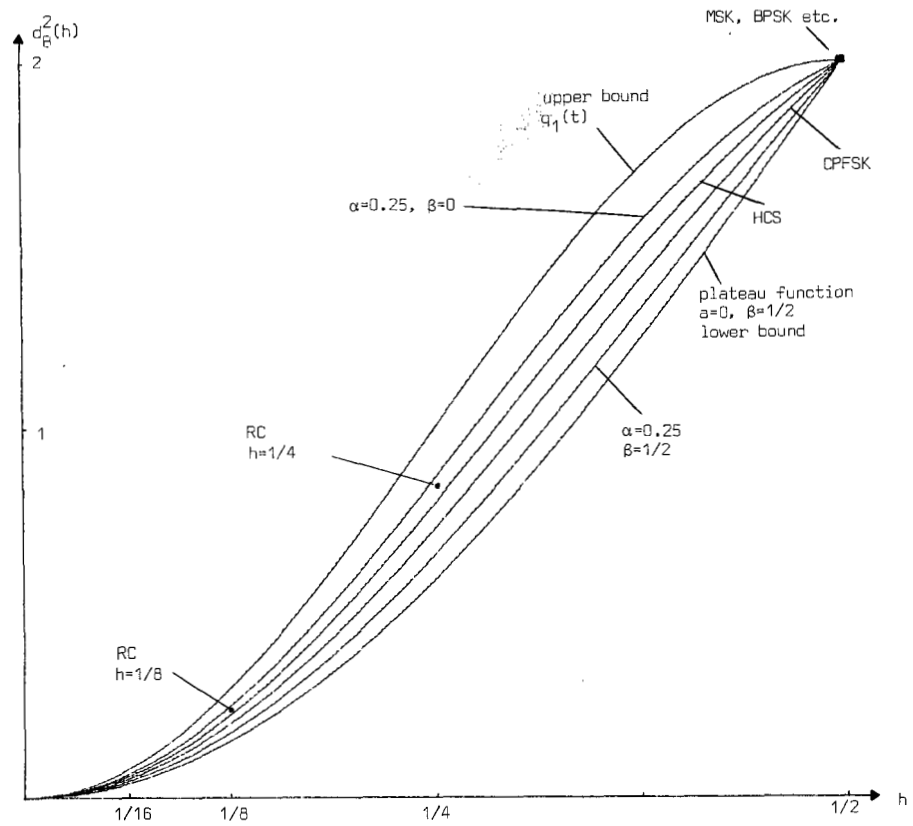

Fig. 5. Upper bound comparison for $M = 2$, $0 \leq h \leq 0.5$. The bound for $q_1(t)$ is the upper bound on all upper bounds $d_B^2(h)$, and the $\alpha = 0$ plateau function is the lower bound on all the upper bounds $d_B^2(h)$ in the considered interval.

This pulse $g(t)$ has one continuous derivative at the end points $t = 0$ and $t = T$. Since this frequency pulse is a raised cosine function, it will be referred to as raised cosine (RC). When $h = 1/2$, this scheme has previously been referred to as SFSK [12].

Fig. 5 shows the upper and lower bounds on $d_B^2(h)$ for all binary schemes in the region $0 \leq h \leq 1/2$, computed with (55). Fig. 5 also shows $d_B^2(h)$ for CPFSK, HCS (with formula in [18]), and α, β functions with $\alpha = 0.25$, $\beta = 0.5$ and $\alpha = 0.25$, $\beta = 0$. The bound for the RC scheme is in between that of $\alpha = 0.25, \beta = 0$ and HCS.

The problem of finding frequency pulses $g(t)$ that optimize $d_B^2(h)$, given h and M, is far more complicated in the general M-ary case than for the binary case. This general problem has not been solved. The reason is that the upper bound is constructed from the minimum of more than one function, and h varies with fixed M, different functions take the minimum value. This is also true for fixed h and M when the frequency pulse $g(t)$ is varied. For an M-ary scheme with $0 \leq h \leq 1/M$ the binary bounds (55) on $d_B^2(h)$ still apply after multiplication with $\log_2 M$.

Of course, also for M-ary schemes $d_B^2(h) \leq 4\log_2 M$. However, due to the fact that the bound $d_B^2(h)$ in this case is formed by taking the minimum of several component functions (32), this maximum value can never be reached [17], [20].

It is previously known [5], [7], that the h-value maximizing the minimum Euclidean distance ($N \geq 3$) for binary CPFSK is $h = 0.715$. This value of h also maximizes $d_B^2(h)$ for this scheme. The same h was also shown by Kotelnikov [1] to maximize the Euclidean distance when $N = 1$. It is possible to find the values of h which maximize $d_B^2(h)$ for M-ary CPFSK [see (33)] and they are given in Table I together with the maximum value of $d_B^2(h)$ for $M = 2, 4, 8, 16$, and 32.

The optimum occurs for h-values slightly below $h = 1$. Unfortunately, $h = 1$ is a first-order weak modulation index for all M, but if N is made large enough ($N \geq N_B$) $d_{\min}^2(h_0)$ equals $d_B^2(h_0)$.

For the quaternary case, the CPFSK scheme gives a maximum of $d_B^2(h_0) = 4.232$. In [17] it is shown that a scheme based on the α, β function with $\alpha = 0$, $\beta = 0.17$ for $h = 0.62$ gives a minimum distance of 4.62. This value came out of a nonexhaustive search for quaternary schemes yielding large distance values. However, better schemes may exist.

IV. NUMERICAL RESULTS ON THE MINIMUM EUCLIDEAN DISTANCE

In this section numerical results on the minimum normalized squared Euclidean distance will be given in form of graphs. These graphs present the minimum Euclidean distance versus the modulation index h for specific schemes and different values of N, the number of received signal intervals observed. Thus, these graphs will show what is below the upper bound $d_B^2(h)$, and also how large N has to be made in a

TABLE I
OPTIMUM h-VALUES AND CORRESPONDING NORMALIZED EUCLIDEAN DISTANCES FOR M-ARY CPFSK SCHEMES

M	Optimum h h_o	$d_B^2(h_o)$	N_B
2	.715	2.434	3
4	.914	4.232	9
8	.964	6.141	41
16	.983	8.088	178
32	.992	10.050	777

specific situation, to make the minimum Euclidean distance $d_{\min}^2(h)$ equal to $d_B{}^2(h)$.

Plateau Functions

As an example of a plateau function, a binary scheme with a phase response very similar to that of $\alpha = 0.05$ and $\beta = 1/2$ will be chosen. The difference between the chosen phase function and the α, β function is that the phase does not vary linearly in the intervals $0 \leqslant t \leqslant \alpha T$ and $(1 - \alpha)\, T \leqslant t \leqslant T$. Instead, the phase varies like a raised cosine (for an exact definition, see b-functions, $b = 0.05$ in [16]).

Fig. 6 shows $d_{\min}^2(h)$ for this binary system. The number of observed bit intervals is $N = 1, 2, \cdots, 7$. The upper bound on the minimum Euclidean distance is also shown by a dashed line where the minimum Euclidean distance still does not equal $d_B{}^2(h)$.

CPFSK and M-ary PSK

Fig. 4 shows the well-known minimum distance for binary CPFSK for $N = 1, 2, 3$, and 4 observed bit intervals. Also shown in Fig. 4 is the upper bound $d_B{}^2(h)$. It can be noted that $h = 1/2$ corresponds to MSK and gives $d_{\min}^2(1/2) = 2$, which is the same as antipodal signaling, e.g., BPSK. The required observation interval for PSK is one bit interval, and for detectors making bit by bit decisions, PSK is optimum [3]. The required observation interval for MSK is two bit intervals, and the asymptotic performance in terms of error probability is the same as that for PSK. The optimum modulation index for CPFSK is $h = 0.715$ when the number of observed symbol intervals is 3. This gives the minimum Euclidean distance $d_{\min}^2(0.715) = 2.43$ and thus a gain of 0.85 dB in terms of E_b/N_0 is obtained compared to MSK or PSK.

The minimum normalized squared Euclidean distance versus the modulation index h is shown in Fig. 7 for the quaternary CPFSK system (see also [10]). Note that the upper bound $d_B{}^2(h)$ (shown by a dashed line where it is not reached) is twice the minimum distance for a receiver observation interval of the $N = 1$ symbol. This is because the rectangular frequency pulse $g(t)$ has the symmetry property (37). The maximum value of $d_B{}^2(h)$ is approximately reached for $N = 8$ observed symbol intervals (compare to Table I).

It is clear from (39) that the first-order weak modulation indexes in the interval $0 \leqslant h \leqslant 2$ are $h_c = 1/3, 1/2, 2/3, 1, 4/3, 3/2, 5/3$, and 2, and the effect of some of these early merges can be clearly seen in Fig. 7. Note that most of these weak

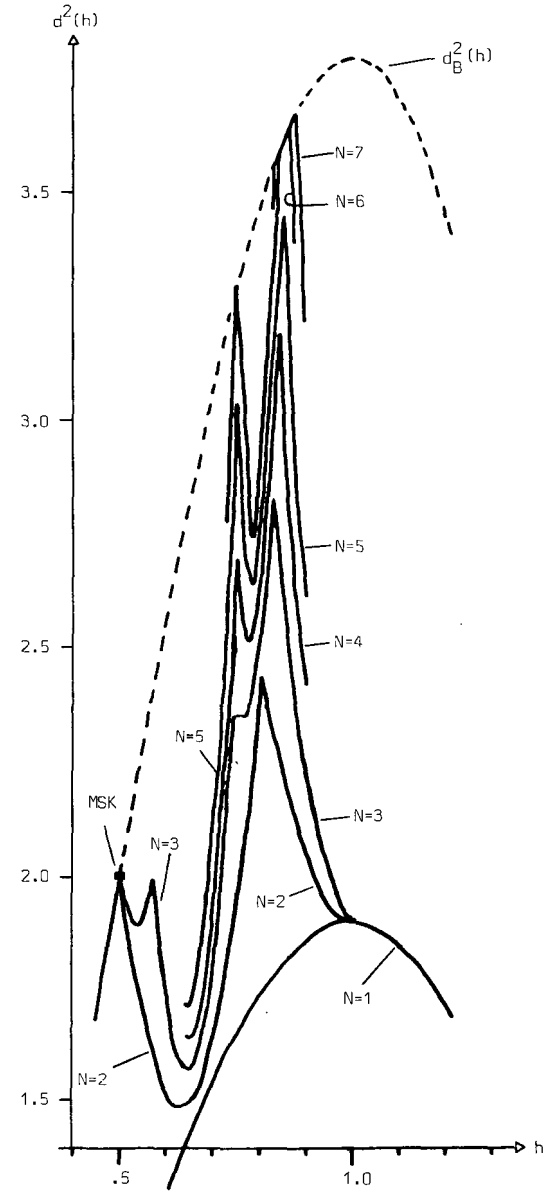

Fig. 6. Normalized squared minimum distances $d^2(h)$ versus modulation index for a b-function with $b = 0.5$. This phase function is very similar to the α-β function with $\alpha = 0.5$, $\beta = 1/2$ (see [16] or [18]).

indexes are catastrophic. The minimum Euclidean distance for these is no better than 2.

It is interesting to compare the minimum distance for the quaternary CPFSK system to QPSK (phase response $q_1(t)$, $h = 1/4$). As indicated in Fig. 7, the minimum squared distance for QPSK is $d_{\min}^2 = 2$, and for the quaternary CPFSK system it is slightly below this value for $h = 1/4$. This is a different relative performance level than that for $M = 2$. For $M = 2$, $h = 1/2$ all schemes have the minimum squared distance $d_{\min}^2 = 2$, CPFSK and PSK included.

The minimum distance for the octal ($M = 8$) CPFSK system is given in Fig. 8 $N = 1, 2, 3$ and in some interval for $N = 4$ and 5. The upper bound $d_B{}^2(h)$, which, as usual, is shown by a dashed line where it is not reached, is like the quaternary case reached with $N = 2$ observed symbol intervals for low

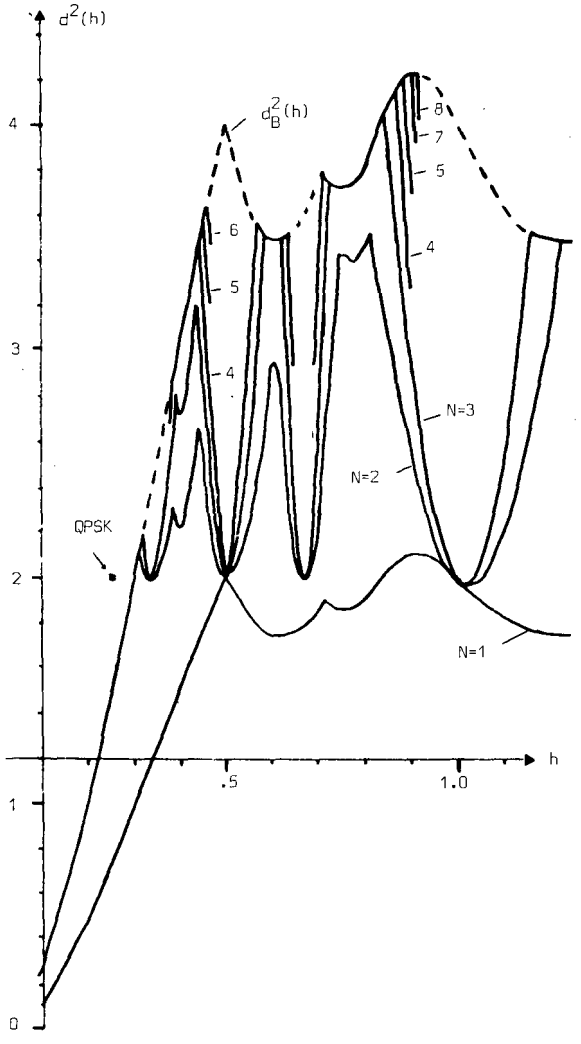

Fig. 7. Minimum normalized squared distance versus modulation index for $M = 4$ CPFSK.

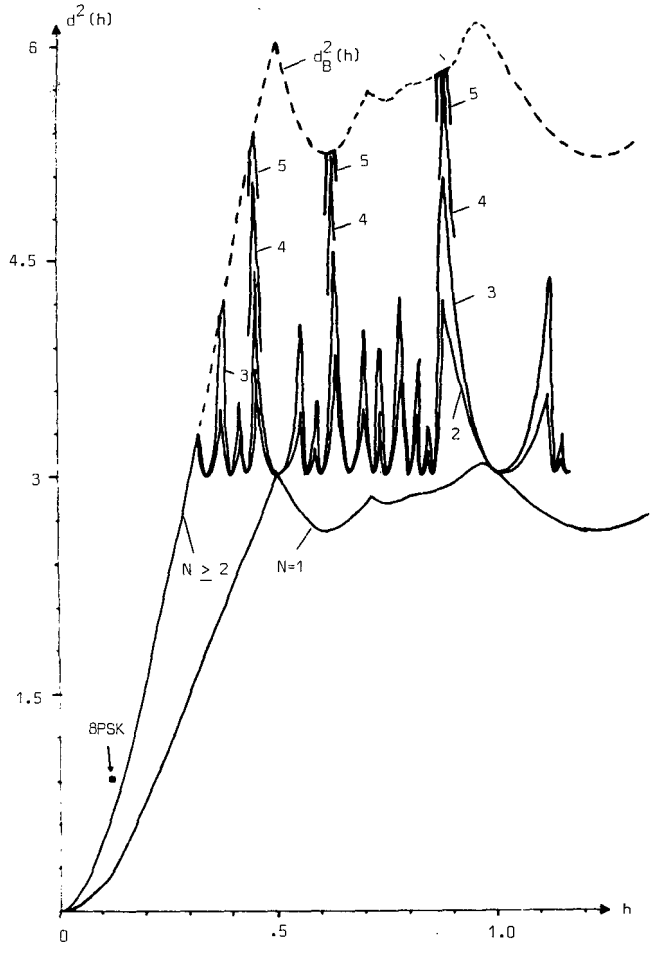

Fig. 8. Minimum normalized squared Euclidean distance versus modulation index for $M = 8$, CPFSK.

modulation indexes. Compared to the quaternary case, the number of first-order weak (catastrophic) modulation indexes has increased in the interval of $0.3 \leqslant h \leqslant 1$. Larger values of N are required to reach $d_B^2(h)$, compared to the quaternary and especially the binary case.

The scheme 8PSK ($q_1(t)$, $h = 1/8$), previously shown to maximize $d_B^2(1/8)$ is also indicated in Fig. 8, and it is seen that octal CPFSK yields the same minimum distance if h is chosen slightly larger than $h = 1/8$ and if $N = 2$. Much larger distances can be obtained for the CPFSK system by choosing, for instance, $h \cong 0.45$ and $N \geqslant 5$.

Distance properties of CPFSK schemes with larger values of M have been investigated in [17], [20]. The maximum attainable minimum distance value grows with M, but the number of first-order weak (castastrophic) modulation index values also grows with M, as does the length of the observation interval necessary for reaching the upper bound $d_B^2(h)$. However, for $h \lesssim 0.3$, $N = 2$ is sufficient for all M. As an illustration to the behavior discussed above, Table I shows N_B which is a lower bound on the observation interval for reaching the upper bound.

HCS, RC, and M-ary PSK

The HCS system yields a phase tree where the phase trajectories are always raised cosine shaped over each symbol interval. Fig. 3 shows the quaternary case.

The upper bound $d_B^2(h)$ for HCS, $M = 2$ is given by [18]

$$d_B^2(h) = 2(1 - \cos \pi h \cdot J_0(\pi h)) \tag{62}$$

where $J_0(\cdot)$ is the Bessel function of the first kind and zero order. The maximum value of $d_B^2(h)$ is smaller than that for binary CPFSK, but this maximum value is still reached with $N = 3$ observed symbols ($d_{\min}^2 = 2.187$ for $h = 0.626$, [18]). For $h = 1/2$, $d_{\min}^2(h)$ equals that of MSK and PSK, as in all binary full response CPM systems. In the region of $0 < h < 1/2$, the upper bound is reached with $N = 2$ observed symbols as in binary CPFSK. Fig. 5 shows that HCS gives a larger minimum distance than binary CPFSK in this region.

The minimum Euclidean distances for the quaternary HSC system are given in Fig. 9 when $N = 1$, 2, 3, and 4 observed symbol intervals, and QPSK is also indicated. $d_B^2(1/4)$ is still smaller than the minimum distance for QPSK of course, but since the upper bound for HCS is reached with $N = 2$ observed symbol intervals in the region of $0 < h \lesssim 0.3$, HCS is better than CPFSK. Note that the value of the minimum Euclidean distance at $h = h_c$ no longer equals 2 as for CPFSK. This is due to

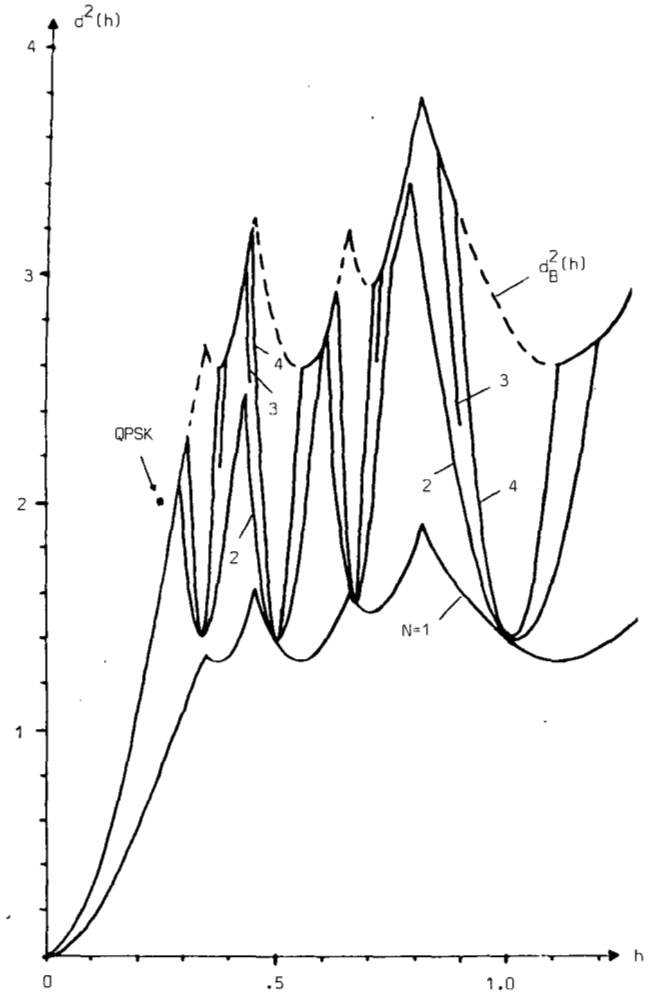

Fig. 9. Minimum normalized squared distance versus modulation index h for $M = 4$, HCS system.

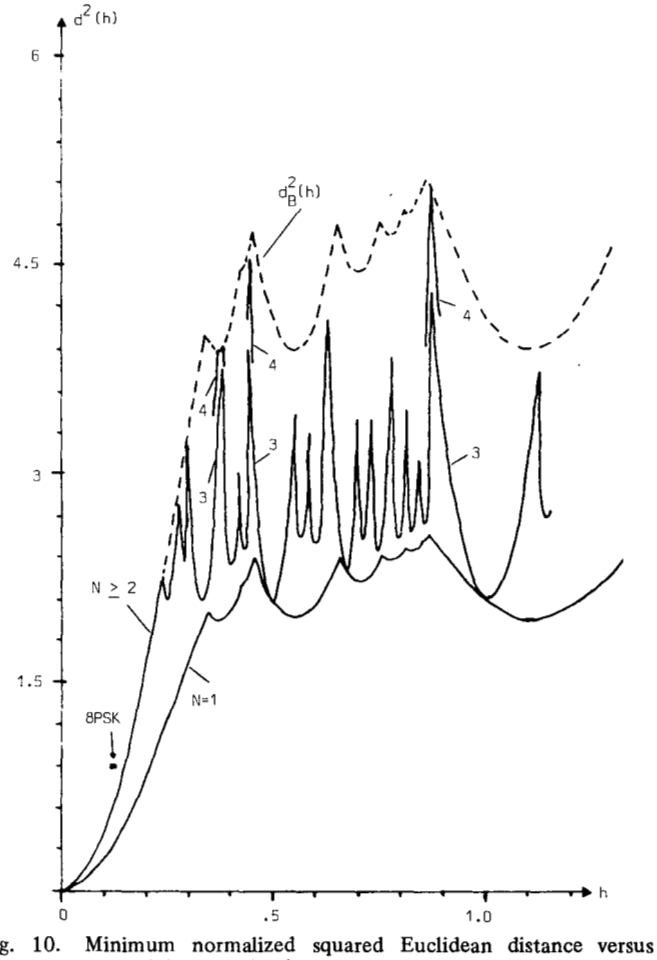

Fig. 10. Minimum normalized squared Euclidean distance versus modulation index h for $M = 8$, HCS system.

the pulse shaping. The results for the octal case (see Fig. 10) follow the same trend as for the CPFSK system; i.e., the upper bound is reached with $N = 2$ for low h-values and the number of catastrophic modulation indexes has increased compared to the quaternary case.

V. POWER SPECTRUM

The power spectral density for the full response CPM schemes considered in this paper can be calculated with formulas given in [2]. The data symbols are assumed to be independent and identically distributed. For the case of full response CPFSK systems, the spectrum can be expressed directly in terms of elementary functions [2] and for *RC* systems in terms of Bessel functions [12].

Spectra for systems with different values of M should be compared at the same bit rate. The bit rate normalized variable $f \cdot T_b$ is used where

$$T_b = \frac{T}{\log_2 M}. \tag{63}$$

Hence, the power spectra $R_0(f)$ are plotted against the bit rate normalized frequency separation from carrier. Plots of the commonly used function [14], [15]

$$P_{0b}(B) = \frac{\int_B^\infty R_0(f)\,df}{\int_0^\infty R_0(f)\,df} \tag{64}$$

which gives the fractional out of band power at the one-sided bandwidth B, will also be given.

Fig. 11 shows the power spectra (double-sided) for M-ary CPFSK with $h = 1/M$, $M = 2, 4, 8$. The corresponding fractional out of band power plots are shown in Fig. 12 (for other values of h, see [17], [20]). It is well known that for fixed M and $g(t)$, the spectrum widens for increasing h. For certain h values discrete components occur. Fig. 11 and the distance figures illustrate the fact that for a roughly fixed distance, the spectral main lobe is decreasing with increasing M. The behavior of the spectra for large frequencies (i.e., the spectral tails) depends only on the number c of continuous derivatives of the instantaneous phase. It is shown in [8] that the tails decrease with f as $|f|^{-2(c+2)}$. For CPFSK, c equals 0.

Fig. 13 shows the spectra for the quaternary CPFSK, HCS, and *RC* schemes for $h = 1/4$. Note that for increased values of c the main lobe becomes larger. The main lobe widens intuitively due to the presence of higher phase slopes over a portion

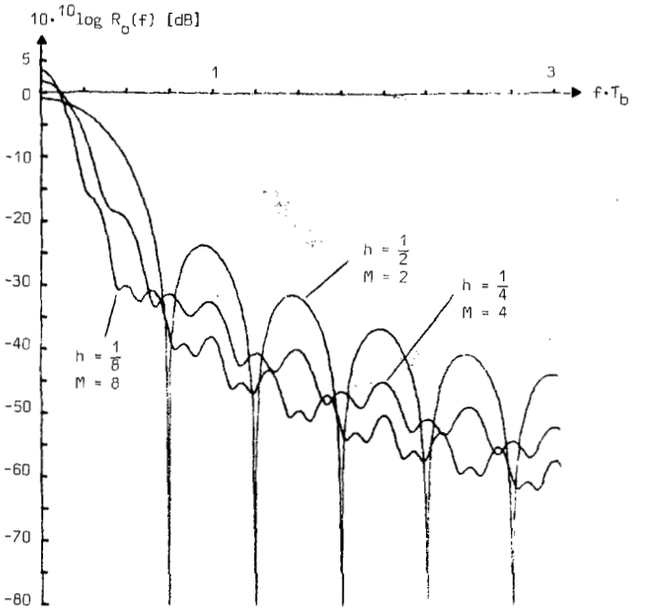

Fig. 11. Normalized power spectral density in decibels for M-ary (M = 2, 4, and 8) CPFSK with modulation indexes H = 1/2, 1/4, and 1/8, respectively.

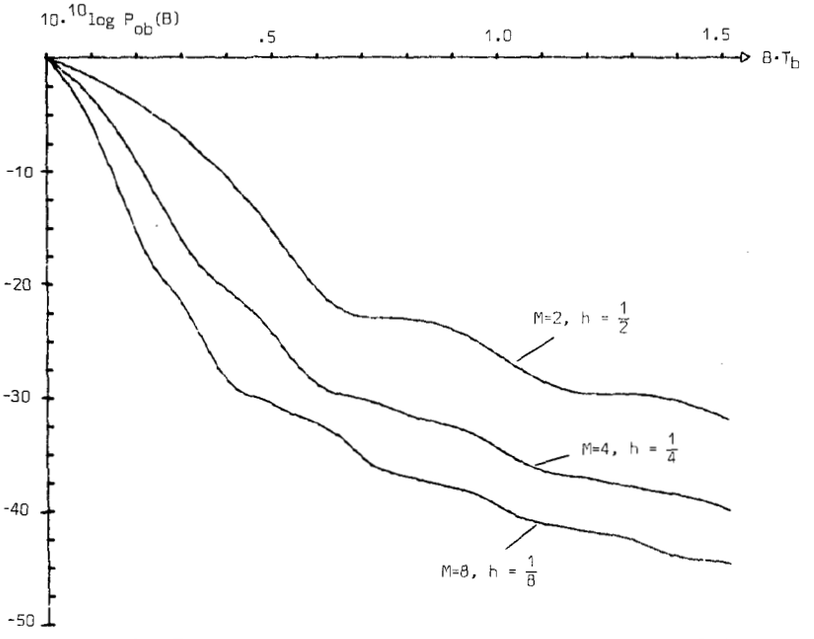

Fig. 12. Fractional out of band power in decibels for M-ary (M = 2, 4, and 8) CPFSK with modulation indexes h = 1/2, 1/4, 1/8, respectively.

of the pulse for non-CPFSK schemes. The spectral tail of HCS behaves like f^{-6} and like f^{-8} for *RC*. Further spectra for these schemes are plotted in [17], [19], [20].

The spectra of schemes with plateau functions are investigated in [16], [18]. As might be expected, the rapid phase change in the beginning and the end of each symbol interval gives wide spectra. The previously mentioned spectral tail behavior versus c is also applicabe in this case. However, f must be impractically large before this asymptotic behavior is dominating. Furthermore, it was concluded above that large $d^2_{\min}$ (close to 4) are reached with plateau functions with $M = 2$ and h close to 1. For $h = 1$, the power spectrum contains spectral lines however.

VI. DISCUSSION AND CONCLUSIONS

From the distance and spectrum results above and in [17], [19], [20], it is evident that M-ary full response CPM schemes have both bandwidth compaction properties and yield gain in E_b/N_0 as compared to MSK. Schemes within this class of CPM systems can also be designed to give a large gain in E_b/N_0 with

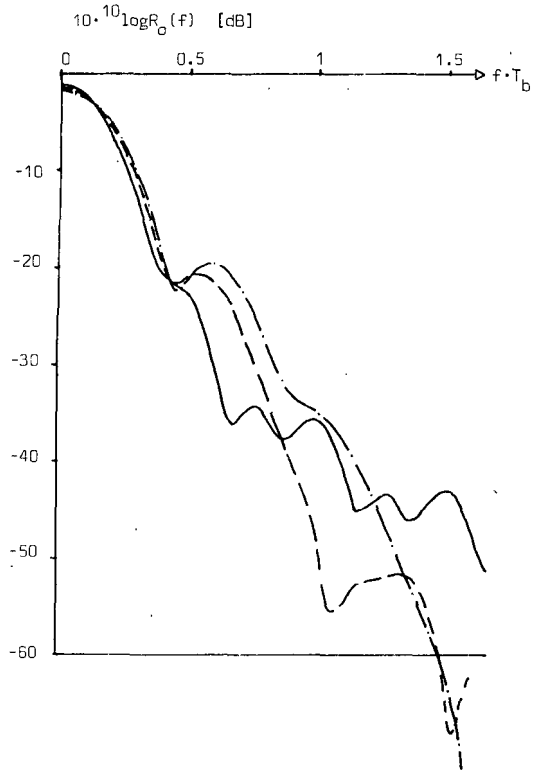

Fig. 13. Normalized power spectral densities in decibles for quaternary CPFSK with modulation index $h = 1/4$. The schemes are CPFSK (solid line), HCS (dashed line), and *RC* (dash-dotted line).

the same bandwidth as MSK, or considerably smaller bandwidth at the expense of an increased E_b/N_0. This holds, for example, for M-ary CPFSK. The same also holds for systems like HCS and *RC*, and in these cases the tradeoff between bandwidth and gain in E_b/N_0 at large SNR is even more attractive.

In the binary case, plateau functions are a way to achieve considerable gains in terms of E_b/N_0, which unfortunately gives poor spectra.

In Table II comparisons between various CPFSK schemes are made, both concerning bandwidth and gain in terms of E_b/N_0 (dB) at large SNR. The reference system is MSK.

Three different definitions of bandwidth will be used. The normalized bandwidth (double-sided) is defined at $2BT_b$, for which 90, 99, or 99.9 percent of the total signal power is within the frequency band $|f - f_0| \leq B$.

Table II also gives the number of observed symbols N_B required to reach the given minimum squared Euclidean distance value. The quaternary scheme with $h = 0.45$ has approximately the same bandwidth as MSK (99 percent bandwidth) and yields a gain in E_b/N_0 of 2.56 dB. The octal scheme with $h = 0.45$ gives a slight bandwidth expansion when compared to MSK (at 99 percent bandwidth), but gives the gain 4.31 dB in terms of E_b/N_0.

A more exhaustive comparison between different M-ary CPFSK systems can be found in Fig. 14. In this figure the gain in decibles of various schemes is shown versus the 99 percent bandwidth. The schems are binary (indicated by x), quaternary (indicated by •) and octal (indicated by □). Note the superior performance of quaternary and octal schemes. In the binary case it was possible to find the frequency pulses $g(t)$ maximizing the upper bound on the minimum Euclidean distance. This was not the case for multilevel systems, and it is believed that the optimum frequency pulse depends on M and h. In the interval $0 < h < 1/M$, M-ary PSK was shown to yield the largest minimum Euclidean distance, but the HCS and *RC* schemes are not far from this optimum. However, the two latter schemes have much smaller spectral tails than M-ary PSK.

It was shown that the number of first-order weak modulation indexes grows with M, thus putting a practical limit on how large an M should be chosen.

TABLE II
BANDWIDTH/DISTANCE TRADEOFF FOR SOME M-ARY CPFSK SYSTEMS

CPFSK scheme	Bandwidth $2B \cdot T_b$			$D^2_{min}/2E_b$	Gain over MSK, dB	N_B symbols
	90%	99%	99.9%			
M=2 h=.5	0.78	1.20	2.78	2.0	0	2
M=4 h=.25	0.42	0.80	1.42	1.45	-1.38	2
M=8 h=.125	0.30	0.54	0.96	.60	-5.23	2
M=4 h=.40	0.68	1.08	2.08	3.04	1.82	4
M=4 h=.45	0.76	1.18	2.20	3.60	2.56	5
M=8 h=.30	0.70	1.00	1.76	3.0	1.76	2
M=8 h=.45	1.04	1.40	2.36	5.40	4.31	5

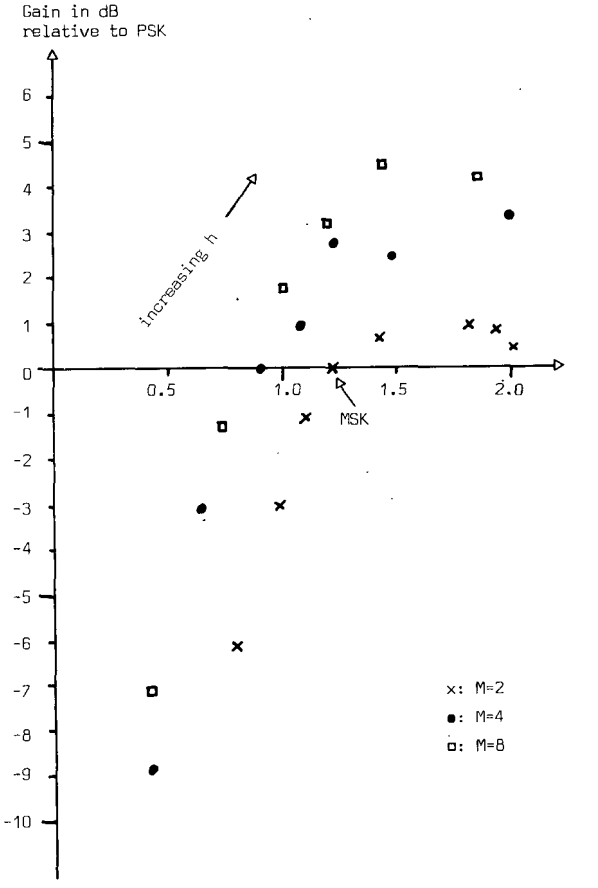

Fig. 14. Bandwidth/performance comparison relative to MSK for various CPFSK systems (99 percent fractional out of band power bandwidth, see Table II).

It is interesting to note that for the schemes considered in this paper, a gain in terms of E_b/N_0 is obtained without expanded bandwidth, compared to MSK. This is different from the case with a channel coded MSK system, where the spectrum must be expanded by a factor of $1/R$ where R is the code rate [3], [9]. For the CPM systems, no parity symbols are transmitted, and the total signal energy is devoted to the information symbols.

This paper explores the distance and bandwidth properties of full response CPM systems. In spite of the restriction that the schemes must be a full response type (i.e., the instantaneous frequency only depends on one data symbol), we have found considerable improvements. However, larger improvements are obtainable with partial response systems (the instantaneous frequency depends on more than one data symbol). This class of system is considered in part II. We have intentionally omitted all problems dealing with transmitter and receiver considerations. These problems will be treated in a unified manner in Part II.

REFERENCES

[1] V. A. Kotelnikov, *The Theory of Optimum Noise Immunity*. New York: Dover, 1960.

[2] R. R. Anderson and J. Salz, "Spectra of digital FM," *Bell Syst. Tech. J.*, vol. 44, pp. 1165–1189, July–Aug. 1965.

[3] J. M. Wozencraft and I. M. Jacobs, *Principles of Communication Engineering*. New York: Wiley, 1965.

[4] R. W. Lucky, J. Salz, and E. J. Weldon, Jr. *Principles of Data Communication*. New York: McGraw-Hill, 1968.

[5] M. G. Pelchat, R. C. Davis, and M. B. Luntz, "Coherent demodulation of continuous phase binary FSK signals," in *Proc. Int. Telemetering Conf.*, Washington, DC, 1971, pp. 181–190.

[6] R. deBuda, "Coherent demodulation of frequency-shift keying with low deviation ratio," *IEEE Trans. Commun.*, vol. COM-20, pp. 429–436, June 1972.

[7] W. P. Osborne and M. B. Luntz, "Coherent and noncoherent detection of CPFSK," *IEEE Trans. Commun.*, vol. COM-22, pp. 1023–1036, Aug. 1974.

[8] T. J. Baker, "Asymptotic behaviour of digital FM spectra," *IEEE Trans. Commun.*, vol. COM-22, pp. 1585–1594, Oct. 1974.

[9] W. C. Lindsey and M. K. Simon, *Telecommunication Systems Engineering*. Englewood Cliffs, NJ: Prentice-Hall, 1974.

[10] T. A. Schonhoff, "Symbol error probabilities for M-ary coherent continuous phase frequency-shift keying (CPFSK)," in *Proc. IEEE Int. Conf. Commun. Conf. Record*, San Francisco, CA, 1975, pp. 34.5–34.8.

[11] T. A. Schonhoff, "Bandwidth vs performance considerations for CPFSK," in *Proc. IEEE National Telecommun. Conf. Record*, 1975, pp. 38.1–38.5.

[12] F. Amoroso, "Pulse and spectrum manipulation in the minimum (frequency) shift keying (MSK) format," *IEEE Trans. Commun.*, vol. COM-24, pp. 381–384, Mar. 1976.

[13] T. A. Schonhoff, "Symbol error probabilities for M-ary CPFSK: Coherent and noncoherent detection," *IEEE Trans. Commun.*, vol. COM-24, pp. 644–652, June 1976.

[14] M. K. Simon, "A generalization of the minimum-shift-keying (MSK)-type signaling based upon input data symbol pulse shaping," *IEEE Trans. Commun.*, vol. COM-24, pp. 845–856, Aug. 1976.

[15] M. Rabzel and S. Pasupathy, "Spectral shaping in minimum shift keying (MSK) type signals," *IEEE Trans. Commun.*, vol. COM-26, pp. 189–195, Jan. 1978.

[16] T. Aulin and C-E. Sundberg, "Binary CPFSK type of signaling with input data symbol pulse shaping—Error probability and spectrum," Telecommunication Theory, Techn. Rep. TR-99, Univ. Lund, Lund, Sweden, July 1978.

[17] ——, "M-ary CPFSK type of signaling with input data symbol pulse shaping—Minimum distance and spectrum," Telecommunication Theory, Techn. Rep. TR-111, Univ. Lund, Lund, Sweden, Aug. 1978.

[18] ——, "Bounds on the performance of binary CPFSK type of signaling with input data symbol pulse shaping," in *Proc. IEEE Nat. Telecommun. Conf. Record*, Birmingham, AL, 1978, pp. 6.5.1–6.5.5.

[19] ——, "M-ary CPFSK type of signaling with input data symbol pulse shaping—Minimum distance and spectrum," in *Proc. IEEE Int. Conf. Commun. Conf. Record*, Boston, MA, 1979, pp. 42.3.1–42.3.6.

[20] T. Aulin, "CPM—A power and bandwidth efficient digital constant envelope modulation scheme," Dr. Techn. dissertation, Telecommunication Theory, Univ. Lund, Lund, Sweden, Nov. 1979.

[21] T. Aulin, N. Rydbeck, and C.-E. W. Sundberg, "Continuous phase modulation—Part II: Partial response signaling," this issue, pp. 210–225.

★

Tor Aulin (S'77–M'80), for a photograph and biography, see this issue, p. 195.

★

Carl-Erik W. Sundberg (S'69–M'75), for a photograph and biography, see this issue, p. 195.